Surface and blood-contacting properties of alkylsiloxane monolayers supported on silicone rubber

James H. Silver,[1,*] Robert W. Hergenrother,[1,†] Jui-Che Lin,[1,‡] Florencia Lim,[1] Horng-Ban Lin,[1,§] Toshiyuki Okada,[2] Manoj K. Chaudhury,[3,‖] and Stuart L. Cooper[4,‖]

[1]Department of Chemical Engineering, University of Wisconsin, Madison, Wisconsin 53706; [2]Dow Corning Corporation, Midland, Michigan 48686; [3]Department of Chemical Engineering, Lehigh University, Bethlehem, Pennsylvania 18015; [4]College of Engineering, University of Delaware, Newark, Delaware 19716

Self-assembled monolayers of alkylsiloxanes supported on polydimethyl siloxane (PDMS) rubber were used as model systems to study the relation between blood compatibility and surface chemistry. The inner lumen of PDMS tubes was first treated with an oxygen plasma. The resultant oxidized surfaces were postderivatized by reacting them with alkyltrichlorosilanes to form the monolayer films. The chemical properties of the monolayers were controlled by varying the head-group chemical compositions. Surface derivatization was verified using variable-angle X-ray photoelectron spectroscopy (XPS or ESCA). Blood compatibility was evaluated using a canine *ex vivo* arteriovenous series shunt model. Surfaces grafted with hydrophobic head-groups as $-CH_3$ and $-CF_3$ had significantly lower platelet and fibrinogen deposition than the surfaces composed of hydrophilic groups such as $-CO_2CH_3$, $-(CH_2CH_2O)_3COCH_3$, and $-(OCH_2CH_2)_3OH$.

INTRODUCTION

One of the central ideas of biomaterials research is that the surface chemistry of an implanted device or material directly affects its hemocompatibility. Thus study is considered incomplete without an evaluation of the surface properties of a given biomaterial. For many of these materials, however, the surface chemistry is quite complex, and it is difficult to be sure of the chemical composition at the blood–biomaterial interface. Many commercially available materials, such as Biomer®, may contain surface-active additives, such as antioxidants or processing aids, which further complicates interpretation of blood–material interactions.[1] Multiphase materials such as polyurethanes may show surface reorientation between the dry and hydrated states,[2] making it difficult to evaluate the surface composition using methods in which the polymer surface is analyzed in air or *in vacuo*.

Many investigators have attempted to modify surfaces of polymers via plasma-processing techniques, to improve their hemocompatibility, without affecting their bulk mechanical properties.[3–5] However, such methods are difficult to control, and while the surface properties may be evaluated subsequent to modification, they cannot be predicted *a priori*. Furthermore, the surface structure of such films may be quite complex, having numerous functional groups and chemical crosslinks.[5] Time-dependent reconstruction of these surfaces may also be observed; the stability of such films is thus of concern.[5]

Recently, much interest has arisen in self-assembled monolayers (SAMs), with the goal of developing molecular-level control over surface properties, both for fundamental studies of surface phenomena and for technological applications.[6–9] These films are typically formed by the adsorption of terminally functionalized alkanethiols $[HS(CH_2)_nX]$ onto gold substrates,[8,10,11] or the adsorption of terminally functionalized silanes onto silicon surfaces, glass, or fused silica.[6,12–17] Formation of SAMs on elastomeric materials such as polydimethyl siloxane (PDMS) has recently been demonstrated as well.[18–20]

The biological interactions of these types of sur-

*Dr. Silver's current address is Prograft Medical Inc., 2400 Faber Place, Palo Alto, CA 94303.

†Dr. Hergenrother's current address is Target Therapeutics, 47201 Lakeview Blvd., Fremont, CA 94537.

‡Dr. J.-C. Lin's current address is Department of Chemical Engineering, National Cheng Kung University, Tainan, Taiwan 70101, ROC.

§Dr. H.-B. Lin's current address is Meadox Medical Corporation, 112 Bauer Dr., Oakland, NJ 07436.

‖Authors to whom correspondence should be addressed.

Journal of Biomedical Materials Research, Vol. 29, 535–548 (1995)

CCC 0021-9304/95/040535-14

faces are now beginning to be investigated. A number of reports have appeared which suggest that the adhesion of cells is profoundly influenced by the chemical properties of self-assembled monolayers.[6,21] Others have used the control provided by SAMs to direct protein adsorption onto such surfaces.[11,16,21,22] However, the interactions between larger, more complex proteins such as fibronectin with SAMs are still difficult to control, which result in a number of different cellular responses.[17] Recently, the adsorption of the tobacco mosaic virus to the domain edges (CH_2 surface) of a Langmuir–Blodgett film composed of hydrocarbon islands in a continuous fluorocarbon sea was reported.[23] To date, however, very little information is available regarding the blood compatibility of such surfaces.

To carefully control the structure of our blood-contacting surfaces, we have functionalized the surface of polydimethyl siloxane (PDMS) in a two-step process, using specific chemistries to form surface monolayers with known compositions. In the first step, the surface is oxidized using an oxygen plasma; in the second step, a self-assembled monolayer is formed by chemisorption of alkyltrichlorosilanes [$Cl_3Si(CH_2)_nR$] onto these surfaces.[18,19] The surface chemistry is controlled by modification of the head group functionalities (R) of these silanes. The resulting functional groups allow us to investigate the interactions between these chemical groups and blood. The functionalities studied are methyl (CH_3), trifluoromethyl (CF_3), ethylene oxide [$(OCH_2CH_2)_3OH$], ester-terminated ethylene oxide [$(CH_2CH_2O)_3COCH_3$], and ester-terminated alkyl chains [$(CH_2)_{11}OCOCH_3$].

The fluorinated groups were chosen for study of the influence of the more highly electronegative fluorine groups, which should result in a polymer with higher interfacial free energy at the water–polymer interface.[24,25] Goretex® vascular grafts are made from expanded polytetrafluoroethylene, and a great deal of clinical experience has been obtained with this material, although they are not used for smaller diameter grafts. Incorporation of fluorine groups by radiation grafting has been performed by Kiaei et al.,[26] Bohnert et al.,[27] and Garfinkle et al.[28] In this study, woven Dacron vascular grafts were modified with a tetrafluoroethylene plasma, and it was found that the hemocompatibility of these materials was significantly improved, compared to untreated materials. *In vitro*, the embolization levels on these surfaces were significantly lower than on controls. Although less fibrinogen was adsorbed on TFE-Dacron, it was more tightly bound to the surface, as determined by elution with sodium dodecyl sulfate. However, this surface shows a variety of functional groups, including CF_3, CF_2, $CF–CF_n$, CF, and $C–CF_n$, as determined from the high-resolution C_{1s} is peak in the ESCA spectrum. Han et al.[25] evaluated the blood compatibility of polyurethanes surface-modified with perfluorodecanoic acid and found that the occlusion times for this material were significantly prolonged.

It has been suggested that surfaces grafted with poly(ethylene oxide) (PEO) are relatively blood compatible.[29,30] This is attributed to the high mobility and low interfacial tension of PEO in an aqueous environment. It was hoped that materials with surface monolayers of ethylene oxide groups might resist thrombosis by inhibiting protein and platelet adhesion.[31,32] Further, by altering the specific terminal group on the ethylene oxide chain from a hydroxyl to an ester, the biocompatibility might be altered.

The effect of head-group chemistry on biocompatibility is investigated by the incorporation of ester-terminal groups, instead of hydroxyl-terminated chains. This change in surface chemistry should allow distinction between surface chemistry and surface mobility.

In this article, the hemocompatibility of a silicone elastomer and surface-derivatized silicone elastomers was evaluated using a canine *ex vivo* series shunt model. Surface characterization of these materials was carried out using X-ray photoelectron spectroscopy and contact angle determination.

EXPERIMENTAL

Materials

Polyethylene tubing (0.125 inch ID) was purchased from Clay-Adams (Intramedic, Parsippany, NJ; Lot 93485). Silicone rubber tubes (0.125 inch ID) (Silastic Pump Grade) and 5 surface-modified Silastic tubes were received from Dow Corning. The inner lumen of the PDMS tubes were silanized according to a modified version of the technique described previously.[18–20]

PDMS tubes about 5 ft long (⅛ inch ID, ¼ inch OD) were evacuated from one end while oxygen was allowed to flow from the other end. The pressure was adjusted to 0.2 mm Hg. A hollow metal spacer was used as an interconnect between the PDMS tube and vacuum system. The oxygen was ionized by connecting the metal spacer to an induction (Tesla) coil. The treatment lasted for 45 seconds. The oxygen plasma generated in this way oxidized the internal surfaces of PDMS tube, as evidenced by its total wetting by water.

These plasma-oxidized PDMS tubes, referred to as $PDMS^{ox}$, were treated with alkyl trichlorosilanes according to the following procedure. Alkyl trichlorosilanes were dissolved in perfluorooctane to final concentrations of 10–20 μg silane/1 g of solvent. The ox-

idized PDMS tubes were filled with these solutions and were allowed to equilibrate for ~2 h. The reason for using perfluorooctane is because this solvent does not swell PDMS. After 2 h of adsorption, the PDMS tubes were washed with fresh perfluorooctane, ethanol, and distilled water. The silanes react with $PDMS^{ox}$ to form the monolayer films. For convenience, we will refer to the silane treated $PDMS^{ox}$ as $PDMS^{ox}$–$O_3Si(CH_2)_nR$. The wettability of the silane-treated tubes altered remarkably as a function of the chemical compositions of the silanes. The surfaces treated with $Cl_3Si(CH_2)_9CH=CH_2$, $Cl_3Si(CH_2)_9CH_3$, and $Cl_3Si(CH_2)_2(CF_2)_7CF_3$ were all hydrophobic (contact angle $\theta_{H_2O} > 90°$), as evidenced by the capillary depression of water, whereas the surfaces treated with $Cl_3Si(CH_2)_{11}CO_2CH_3$ and $Cl_3Si(CH_2)_3(OCH_2CH_2)_3OCOCH_3$ became hydrophilic. The olefin-terminated PDMS surface ($PDMS^{ox}$–$O_3Si(CH_2)_9CH=CH_2$) was further reacted with $HS(CH_2)_3(OCH_2CH_2)_3OH$ by a free radical process to introduce the ethylene oxide functionality to the surface as shown:

$$PDMS^{ox}\text{–}O_3Si(CH_2)_9CH=CH_2 + HS(CH_2)_3(OCH_2CH_2)_3OH \xrightarrow{\text{Benzephenone and UV light}} PDMS^{ox}\text{–}O_3Si(CH_2)_{11}S(CH_2)_3(OCH_2CH_2)_3OH$$

$PDMS^{ox}$–$O_3Si(CH_2)_9CH=CH_2$ tubes were filled with an ethanolic solution of $HS(CH_2)_3(OCH_2CH_2)_3OH$ (2 wt%) and benzophenone (0.15 wt%) and then exposed to mercury UV light for 5 min. Benzophenone abstracts the proton from the thiol to generate free radicals, which are readily inserted into the olefin groups.

Surface property characterization

X-ray photoelectron (XPS or ESCA) spectra were obtained using a Perkin-Elmer Physical Electronics PHI 5400 spectrometer. Samples of each tube were cut in half lengthwise, and flattened to hold them onto the sample stage. A magnesium anode operating at 300 W and 15 kV and photoelectron emission angles of 30, 45, and 60° were used. High-resolution spectra of the O_{1s} peak, N_{1s} peak, C_{1s} peak, Si_{2p} peak, and F_{1s} peak were collected at a pass energy of 17.9 eV using a 1000-μm diameter X-ray spot size. The relative atomic percentage of each element at the surface was estimated from the peak areas using atomic sensitivity factors specified for the PHI 5400. The high-resolution C_{1s} spectra were curve-fit to analyze the chemical bonding states of the carbon atoms. A variable combination of Gaussian and Lorentzian peak shapes were used to fit the peaks. Data analysis and C_{1s} peak fitting was performed using software provided by Perkin-Elmer. Inversion of the angle-dependent ESCA data was done using a computer program supplied by Dr. B. J. Tyler (University of Washington).[33] Inversion of the angle-dependent ESCA data requires that the photoelectron inelastic mean free paths for each element be known. These were determined using the equation of Seah and Dench.[34]

Water-in-air static contact angles were measured on the concave inner lumen of these surfaces using the method of Lelah et al.[35] Short tubes of PDMS were cut into hemicylindrical form. Small drops (ca. 1 mm) of water were placed on the inner lumen of these tubes, and were either photographed or analyzed by a video microscopy system. Tangent lines were drawn at the intersection of the drop and the PDMS surface by geometric construction directly on the photograph or on a replica of the video image to estimate the contact angles.

Blood-contacting properties

The blood-contacting properties of these materials were evaluated using a canine *ex vivo* series shunt experiment,[36] with modifications described by Grasel and Cooper[37] (Fig. 1). The polymer tubings were cut into 1.5-inch lengths and assembled into shunts. Each polymer was present in triplicate in each shunt.

Adult mongrel dogs, which were selected after hematologic screening, were injected with autologous

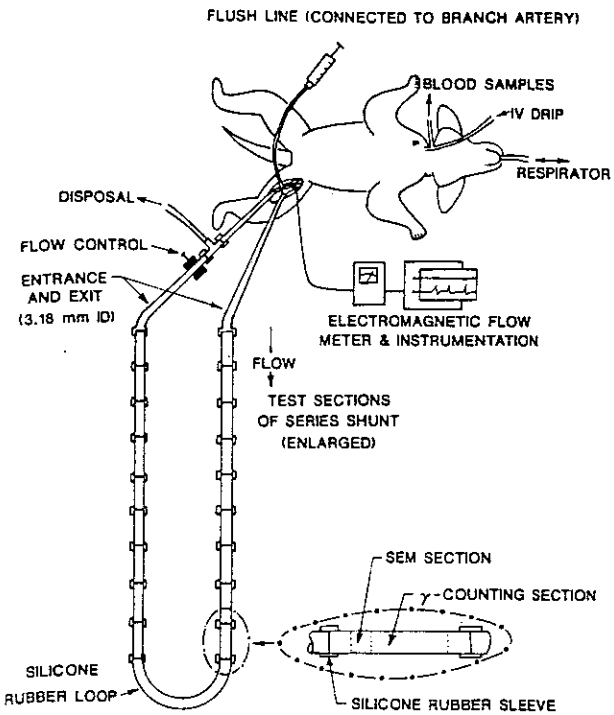

Figure 1. Schematic diagram of canine series shunt experiment showing shunt details in an expanded scale.

^{111}In-labeled platelets and ^{125}I-labeled fibrinogen. No anticoagulants were used in this procedure. The shunts were filled with sterile, degassed, divalent cation-free Tyrodes solution (0.2 g/l KCl, 8.0 g/l NaCl, 0.05 g/l NaH_2PO_4–H_2O, 1.0 g/l dextrose, 1.0 g/l $NaHCO_3$, pH 7.35), and hydrated overnight at 4°C. The femoral artery and vein were cannulated with the shunt. A branch artery proximal to the shunt cannulation site was connected to a flushing system. The blood flow rate was continuously monitored during blood exposure using an electromagnetic flow probe. The initial flow rate was controlled at 280 ± 20 ml/min. Blood samples were collected hourly to determine bulk radioactivity, platelet and fibrinogen concentrations, hematocrit, blood gas analysis, and hematologic function.

Three separate surgeries were performed. Shunts were run for 1, 2, 5, 10, 15, 20, 25, 30, 45, and 60 min of blood contact. At the end of each blood contact interval, the femoral artery was clamped, and the bulk blood was flushed out of the shunt at a flow rate of approximately 60 ml/min, which gives a much lower shear rate than that during blood contact. Immediately following flushing, the test sections were removed, and the tube contents were fixed with 2% glutaraldehyde. Then, test sections were subdivided into sections for γ-scintillation counting and for evaluation by scanning electron microscopy (SEM). Samples were prepared for scanning electron microscopy using the procedure previously described.[38] These samples were examined using a JEOL JSM-35C SEM at 15 kV accelerating voltage.

Platelet and fibrinogen deposition profiles were determined by counting the segments in a γ-counter (Gamma 5500; Beckman) and converting the number of counts into the number of platelets or mass of fibrinogen. The average and standard deviation of the nine data points (three data points for each of three surgeries) was obtained. Outlier data points among the nine points were rejected at the 95% confidence level, using Nalimov's test.[39] Negative values (primarily fibrinogen data at short times) were set to zero.

RESULTS AND DISCUSSION

Surface characterization

Concentration–depth profiles obtained for materials studied are shown in Figures 2–7. Similar concentration–depth profiles were noticed for PDMS^{ox}–$O_3Si(CH_2)_3(OCH_2CH_2)_3OCOCH_3$ and PDMS^{ox}–$O_3Si(CH_2)_{11}S(CH_2)_3(OCH_2CH_2)_3OH$ surfaces as those for PDMS^{ox}–$O_3Si(CH_2)_{11}CO_2CH_3$. The surface-derivatized materials each show depth profiles for silicon which are comparable with the Silastic pump grade tubing. This result indicates that the surface-treatment process does not penetrate significantly into the bulk. No measurement of the surface thickness on these PDMS elastomers has been made. It is also not known how homogeneous these surfaces are, nor was information obtained about the size or nature of any defects. All of the materials show a

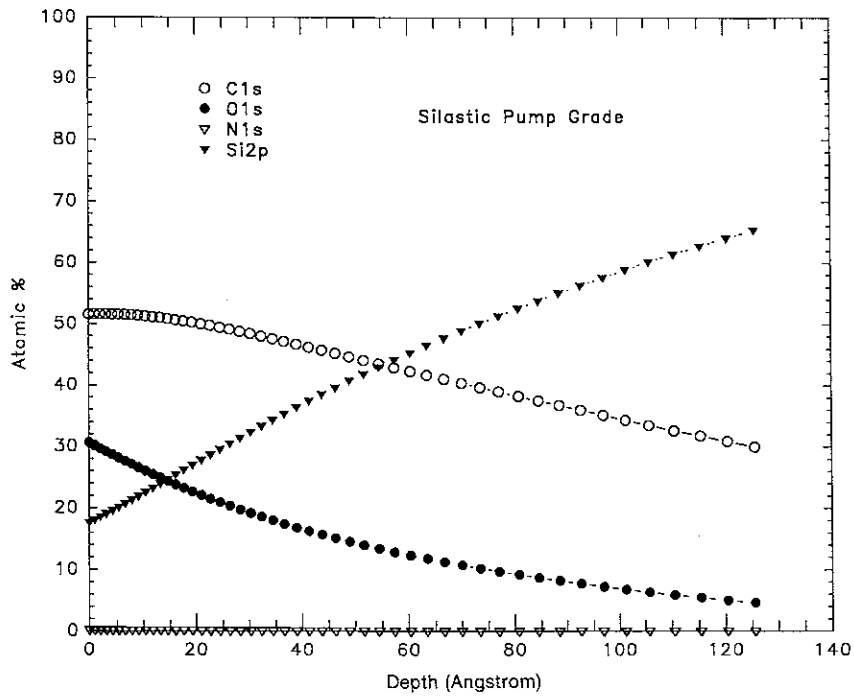

Figure 2. ESCA concentration–depth profile for Silastic pump grade tubing.

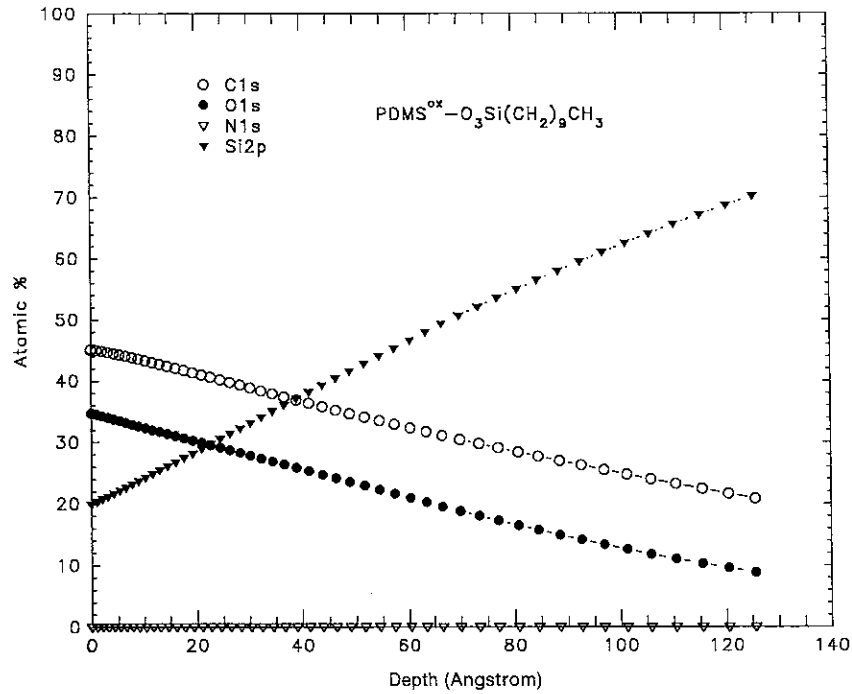

Figure 3. ESCA concentration–depth profile for PDMS^{ox}–$O_3Si(CH_2)_9CH_3$.

decrease in C_{1s} and O_{1s} signals going from the surface to the bulk. The derivatized materials show about 5–10% more O_{1s} than Silastic pump grade tubing, but about 5–15% less C_{1s} than this material. The increased oxygen content and decreased carbon content may be due to loss of the monolayer, as the tubes were flattened for ESCA analysis and may have exposed some of the underlying PDMS material.

Incorporation of these new functional groups onto the surface is supported by the ESCA data. For PDMS^{ox}–$O_3Si(CH_2)_2(CF_2)_7CF_3$, fluorine incorporation provides a marker for the surface derivatization. PDMS^{ox}–$O_3Si(CH_2)_2(CF_2)_7CF_3$ shows multiple C_{1s} peaks, and hence multiple bonding states for the carbon atom. For the other surfaces except for Silastic or PDMS^{ox}–$O_3Si(CH_2)_9CH_3$, changes in the C_{1s} bonding

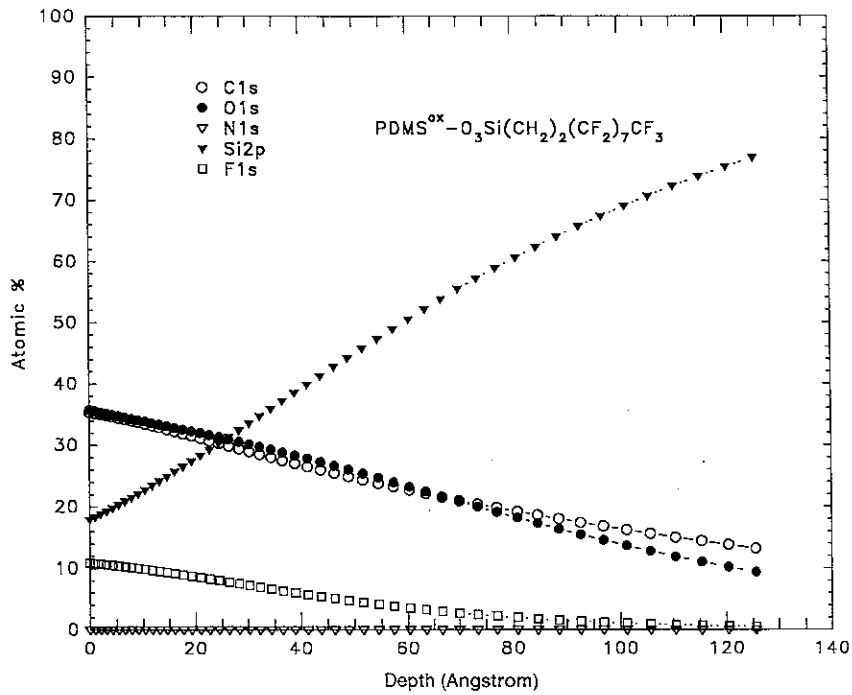

Figure 4. ESCA concentration–depth profile for PDMS^{ox}–$O_3Si(CH_2)_2(CF_2)_7CF_3$.

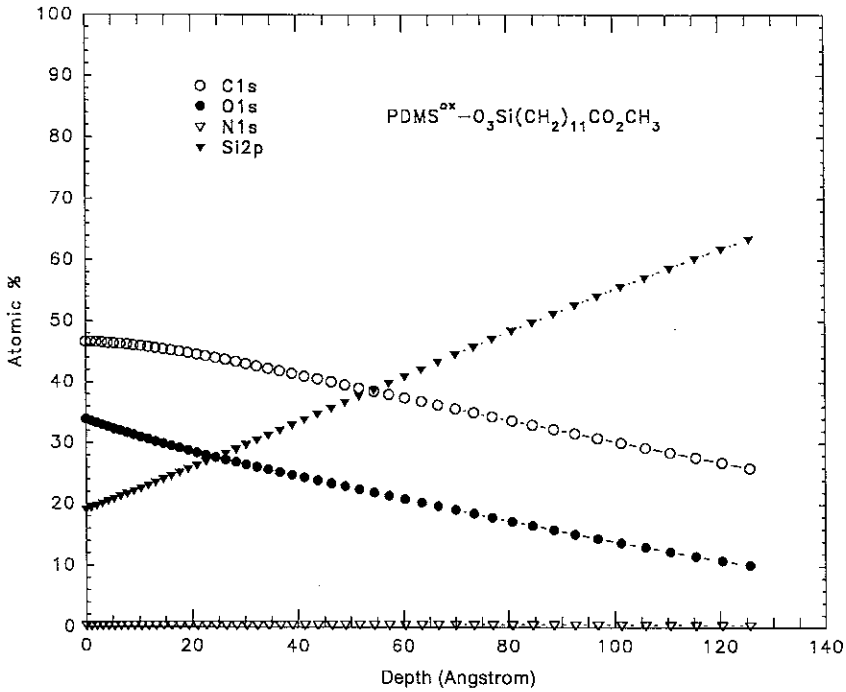

Figure 5. ESCA concentration–depth profile for PDMS^{ox}–$O_3Si(CH_2)_{11}CO_2CH_3$.

state are observed, as shown in Table I, indicating that the new functional groups have been incorporated onto the surfaces. Surfaces derivatized with either PDMS^{ox}–$O_3Si(CH_2)_{11}CO_2CH_3$ or PDMS^{ox}–$O_3Si(CH_2)_3(OCH_2CH_2)_3OCOCH_3$ show the presence of hydrocarbon, ether carbon, and carbonyl carbon groups. PDMS^{ox}–$O_3Si(CH_2)_{11}S(CH_2)_3(OCH_2CH_2)_3OH$ shows the presence of hydrocarbon and ether carbon peaks, but not carbonyl peaks, as expected. No change in C_{1s} bonding state between the Silastic pump grade tubing and the PDMS^{ox}–$O_3Si(CH_2)_9CH_3$-derivatized surface was observed, although derivatization may be inferred since there was a decrease in the C_{1s} content and an increase in the O_{1s} content of the latter material as compared to the unoxidized PDMS.

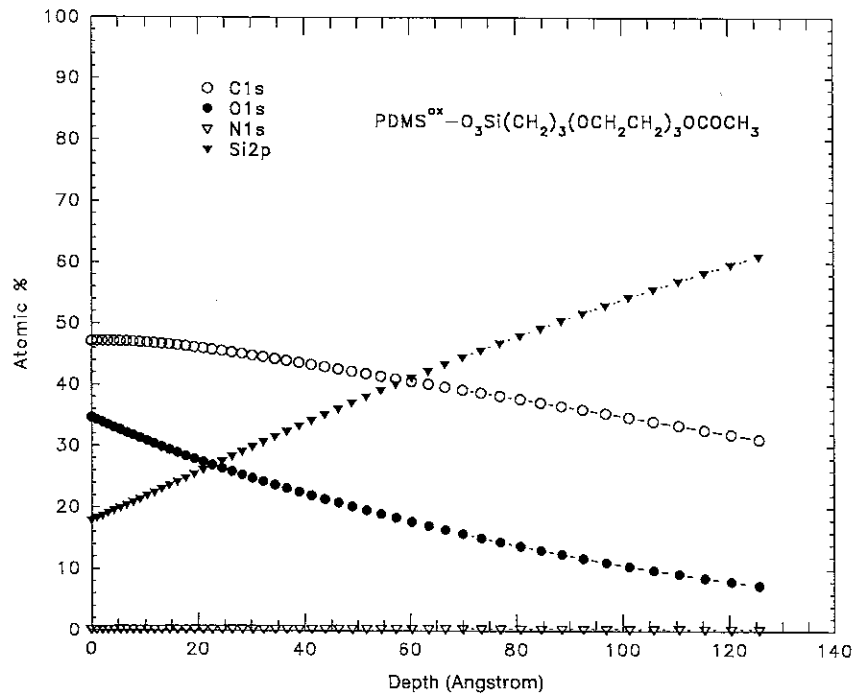

Figure 6. ESCA concentration–depth profile for PDMS^{ox}–$O_3Si(CH_2)_3(OCH_2CH_2)_3OCOCH_3$.

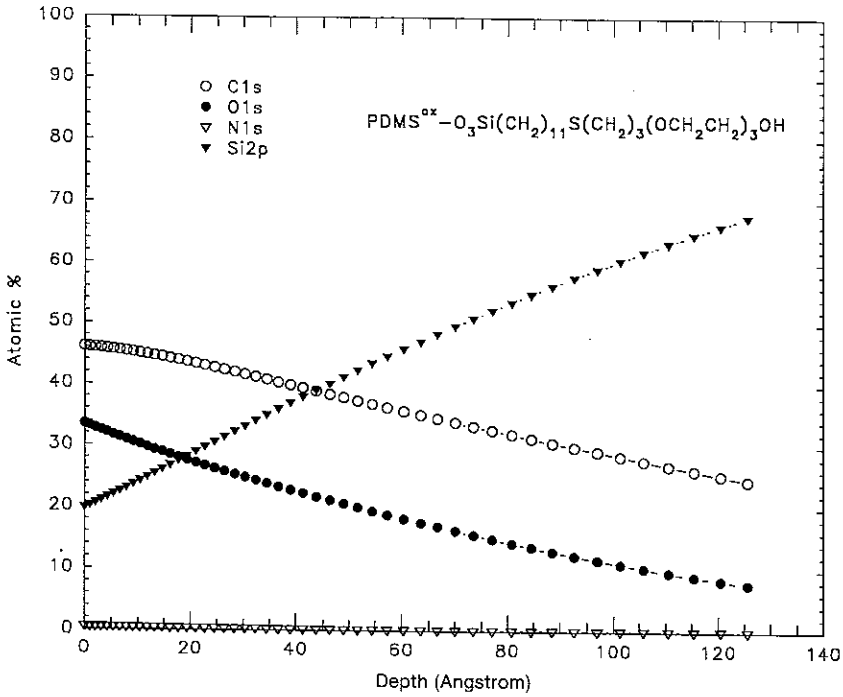

Figure 7. ESCA concentration–depth profile for PDMS^{ox}–$O_3Si(CH_2)_{11}S(CH_2)_3(OCH_2CH_2)_3OH$.

Static contact angle data obtained on these surfaces are shown in Table II. Both PDMS^{ox}–$O_3Si(CH_2)_9CH_3$ and PDMS^{ox}–$O_3Si(CH_2)_2(CF_2)_7CF_3$ were rendered hydrophobic by the surface treatment. The remaining surfaces are found to be much less hydrophobic, the order of hydrophilicity being PDMS^{ox}–$O_3Si(CH_2)_3(OCH_2CH_2)_3OCOCH_3$ > PDMS^{ox}–$O_3Si(CH_2)_{11}S(CH_2)_3(OCH_2CH_2)_3OH$ > PDMS^{ox}–$O_3Si(CH_2)_{11}CO_2CH_3$. However, the differences in hydrophilicity in the latter group are much less than the one between this group and surfaces containing the methyl- and perfluoromethyl terminal units.

We do not have any direct evidence of either the thickness or the structural order of these adsorbed films, but based on the following arguments, we feel that the adsorbed films of alkylsiloxanes expose their terminal functionalities (–CH_3, –CF_3, etc.) in such a way as to affect the chemistry and wettabilities of the surfaces significantly.

To develop the needed argument, let us take the case of PDMS^{ox}–$O_3Si(CH_2)_9CH_3$. A well-ordered film of methyl-terminated silane exposes primarily the –CH_3 groups. The contact angles of water and hexadecane on such a decyl alkyl siloxane film are generally about 110–112 and 38–40°, respectively. If the monolayer is more disordered, it exposes the –CH_2– groups, making it ultimately wettable by hexadecane. The contact angles of water and hexadecane in the present case are found to be 109 ± 2° and 33 ± 3°, respectively. These angles are somewhat lower than those seen on a well-ordered monolayer film. However, if the monolayer were totally disordered, as would be the case for fractional monolayer or multilayers, the monolayer films would expose –CH_2– groups, making them wettable by hexadecane. These observed contact angles indicate that the monolayers are reasonably oriented exposing the –CH_3 groups, but less ordered than the corresponding films found

TABLE I
C1s Peak Fits from ESCA Data

Material	% C–C, C–Si (285 eV)	% C–O (287 eV)	% C=O (289 eV)	% –$(CF_2)_n$– (295 eV)	% –(CF_3) (297 eV)
Silastic pump grade tubing	100.0				
PDMS^{ox}–$O_3Si(CH_2)_9CH_3$	100.0				
PDMS^{ox}–$O_3Si(CH_2)_2(CF_2)_7CF_3$	14.9	57.1*	7.9†	15.0	5.1
PDMS^{ox}–$O_3Si(CH_2)_{11}CO_2CH_3$	93.1	5.3	1.6		
PDMS^{ox}–$O_3Si(CH_2)_3(OCH_2CH_2)_3O$ $COCH_3$	94.4	4.1	1.5		
PDMS^{ox}–$O_3Si(CH_2)_{11}S(CH_2)_3(OCH_2CH_2)_3OH$	92.0	8.0			

*Equivalent to CH_2 in CF_2CH_2.
†Equivalent to CF_2 in CF_2CH_2.

TABLE II
Water-in-Air Contact Angles on PDMS^{ox}–$O_3Si(CH_2)_nR$

Material	Contact Angle
Silastic pump grade tubing	108.5 ± 1.3
PDMS^{ox}–$O_3Si(CH_2)_2(CF_2)_7CF_3$	113.6 ± 3.0
PDMS^{ox}–$O_3Si(CH_2)_9CH_3$	109.2 ± 2.3
PDMS^{ox}–$O_3Si(CH_2)_{11}CO_2CH_3$	66.2 ± 2.8
PDMS^{ox}–$O_3Si(CH_2)_{11}S(CH_2)_3(OCH_2CH_2)_3OH$	59.6 ± 2.3
PDMS^{ox}–$O_3Si(CH_2)_3(OCH_2CH_2)_3OCOCH_3$	54.2 ± 3.0

$n = 5$.

on silicon wafer. It should be noted that the contact angles of the other monolayers varied in an expected way in response to the chemical composition of the terminal groups. For example, the water contact angle of a $-CF_3$ surface was about 114°, which is close to the value observed for other similar films.[9] Similarly, the water contact angle (66°) of a $-CO_2CH_3$ surface[40] is close to the value (73°) reported for a well-ordered film of analogous silane. Other evidence for the orientation of these monolayers comes from the reactivity of the olefin-terminated silane. Although hydrophobic, this monolayer reacts readily with ethylene oxide functional thiols. The resultant surface is hydrophilic ($\theta_{H_2O} \sim 60°$). In the literature,[22] contact angles of ethylene oxidize functional monolayers have been reported to be ~40°. The higher contact angle (60°) observed here may indicate that the free radical reaction does not proceed in a clean or quantitative way. However, we found that the surfaces with longer ethylene oxide chain [$-(OCH_2CH)_4-OH$] is a bit more hydrophilic ($\theta_{H_2O} \sim 50°$) (unpublished results) than the present surface. It may be possible to make the surface more hydrophilic by using longer ethylene oxide chain, but such an attempt has not been made here.

In summary, the wettabilities and reactivity of these monolayers indicate that the molecules adsorb in a way so as to expose the relevant functionalities accessible for the studies of blood-contacting properties reported here. We understand the need to develop appropriate experimental tools to measure directly thickness, as well as other physical properties of these films.

Blood-contacting properties

A material is considered to be thrombogenic if relatively large numbers of platelets and fibrinogen/fibrin molecules adhere to the surface during blood contact. A surface coverage of approximately 70–100 platelets/1000 μm^2 represents a monolayer of platelets on the surface, although the degree of platelet spreading and activation can cause this number to vary.[41]

Figure 8 shows the transient platelet deposition profiles for the materials tested during the initial hour of blood exposure. The platelet deposition profiles show a peak between 10 and 30 min of blood contact. The same trend was previously reported for different polymeric materials in the same canine *ex vivo* series shunt experiment. This peak reflects thrombus growth in competition with embolization. The Silastic pump grade tubing, PE, PDMS^{ox}–$O_3Si(CH_2)_2(CF_2)_7CF_3$, and PDMS^{ox}–$O_3Si(CH_2)_9CH_3$ all had very low levels of platelet deposition, as seen in Figure 8a. Figure 8b shows that PDMS^{ox}–$O_3Si(CH_2)_3(OCH_2CH_2)_3OCOCH_3$ had a higher level of platelet deposition, with a maximum of about 700 platelets/1000 μm^2 at 30 min. Samples derivatized with PDMS^{ox}–$O_3Si(CH_2)_{11}CO_2CH_3$ and PDMS^{ox}–

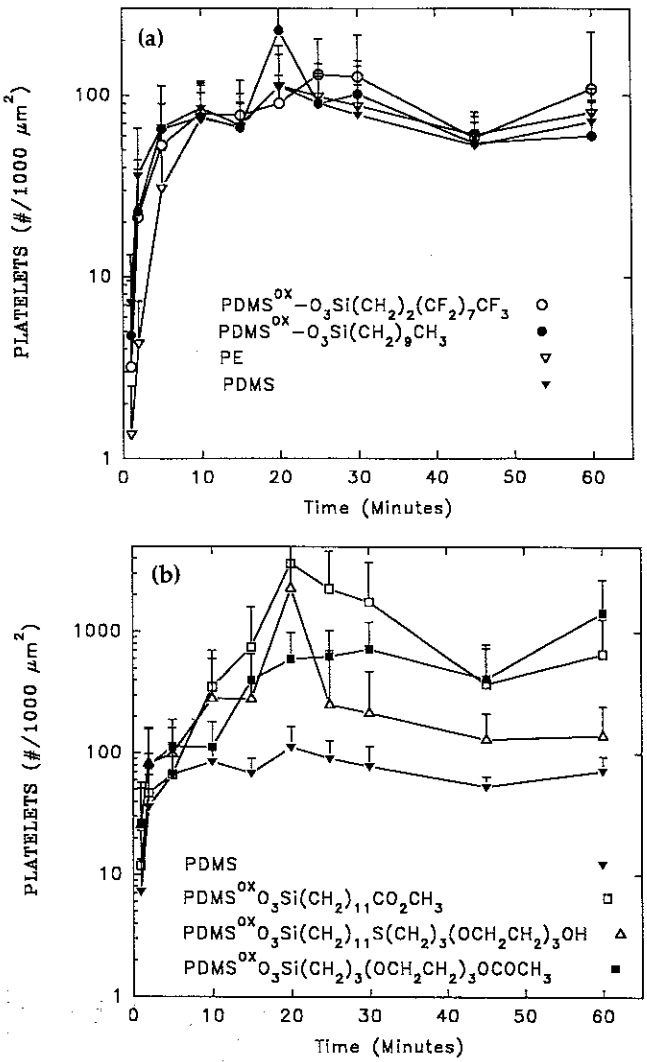

Figure 8. Platelet deposition profiles during the initial hour of blood contact for: (a) PDMS^{ox}–$O_3Si(CH_2)_2(CF_2)_7CF_3$ (open circle); PDMS^{ox}–$O_3Si(CH_2)_9CH_3$ (solid circle); PE (open inverted triangle); PDMS (solid inverted triangle); and (b) PDMS (solid inverted triangle); PDMS^{ox}–$O_3Si(CH_2)_{11}CO_2CH_3$ (open square); PDMS^{ox}–$O_3Si(CH_2)_3(OCH_2CH_2)_3OCOCH_3$ (solid square); PDMS^{ox}–$O_3Si(CH_2)_{11}S(CH_2)_3(OCH_2CH_2)_3OH$ (open triangle).

$O_3Si(CH_2)_{11}S(CH_2)_3(OCH_2CH_2)_3OH$ both had the highest levels of platelet deposition, with peak values of about 3500 and 2000 platelets/1000 μm^2, respectively, after 20 min of blood exposure.

The fibrinogen/fibrin deposition profiles for these materials are shown in Figure 9a and b. Silastic pump grade tubing (PDMS), PE, $PDMS^{ox}$–$O_3Si(CH_2)_2(CF_2)_7CF_3$, and $PDMS^{ox}$–$O_3Si(CH_2)_9CH_3$ had the lowest levels of deposition, as seen in Figure 9a, while $PDMS^{ox}$–$O_3Si(CH_2)_{11}CO_2CH_3$ and $PDMS^{ox}$–$O_3Si(CH_2)_3(OCH_2CH_2)_3OCOCH_3$ both had the highest levels of fibrinogen deposition, followed by $PDMS^{ox}$–$O_3Si(CH_2)_{11}S(CH_2)_3(OCH_2CH_2)_3OH$, as seen in Figure 9b. The fibrinogen/fibrin profiles closely parallel the platelet deposition profiles for all of the materials tested. The similarity in the trends of the platelet and fibrinogen/fibrin deposition profiles indicates fibrinogen incorporation into the thrombi, possibly by blinding to specific platelet membrane receptor sites, or by incorporation into the thrombi as fibrin strands linking the platelets together.[42]

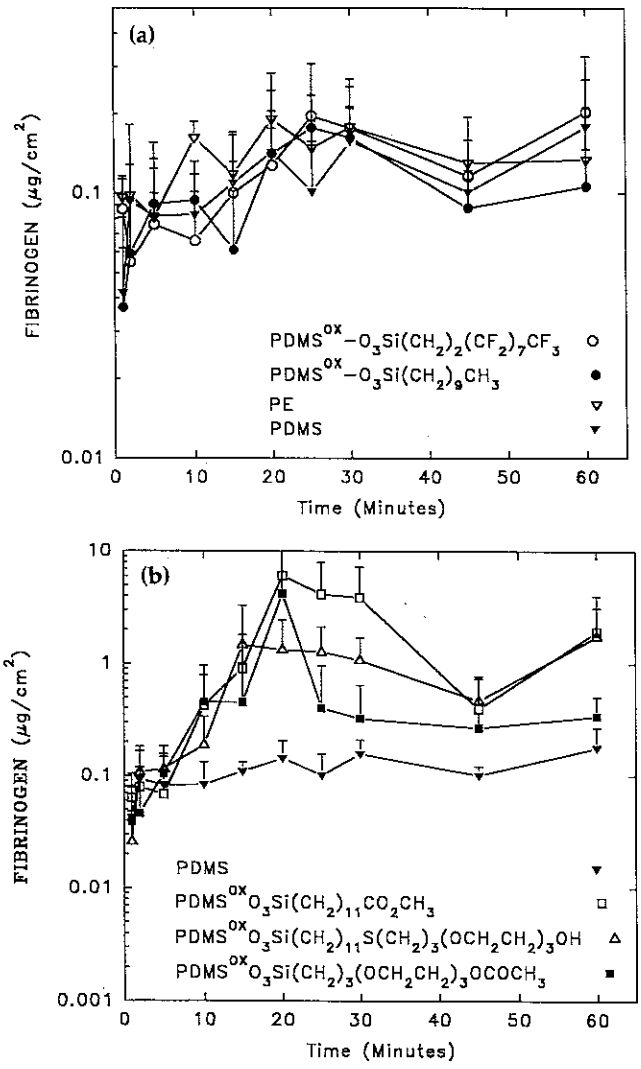

Figure 9. Fibrinogen/fibrin deposition profiles during the initial hour of blood contact for: (a) $PDMS^{ox}$–$O_3Si(CH_2)_2(CF_2)_7CF_3$ (open circle); $PDMS^{ox}$–$O_3Si(CH_2)_9CH_3$ (solid circle); PE (open inverted triangle); PDMS (solid inverted triangle); and (b) PDMS (solid inverted triangle); $PDMS^{ox}$–$O_3Si(CH_2)_{11}CO_2CH_3$ (open square); $PDMS^{ox}$–$O_3Si(CH_2)_3(OCH_2CH_2)_3OCOCH_3$ (solid square); $PDMS^{ox}$–$O_3Si(CH_2)_{11}S(CH_2)_3(OCH_2CH_2)_3OH$ (open triangle).

A ranking of the thrombogenicity of the materials was calculated for each material at each time point for both the platelet and fibrinogen deposition. A relative rank was assigned (highest = 7 and lowest = 1) to each material at each blood-contacting time, and the relative ranks at all blood-contacting times were averaged for each material. Table III summarizes the platelet and fibrinogen ranks for the materials tested. Table III also shows the same trends as Figures 8 and 9, namely, that $PDMS^{ox}$–$O_3Si(CH_2)_{11}CO_2CH_3$, $PDMS^{ox}$–$O_3Si(CH_2)_{11}S(CH_2)_3(OCH_2CH_2)_3OH$, and $PDMS^{ox}$–$O_3Si(CH_2)_3(OCH_2CH_2)_3OCOCH_3$ are the most thrombogenic, and that Silastic pump grade tubing, PE, $PDMS^{ox}$–$O_3Si(CH_2)_2(CF_2)_7CF_3$, and $PDMS^{ox}$–$O_3Si(CH_2)_9CH_3$ had the lowest levels of platelet and fibrinogen deposition. This unweighted rank test does not differentiate between materials which are extremely thrombogenic at the thromboembolytic peak and those which show only slightly greater platelet deposition at early time points. While the former is significant, the latter is a less important indicator of the thrombogenic potential of the material.

Using scanning electron microscopy to observe platelet and thrombus deposition on the surfaces it appeared that the ester-terminated groups seemed to be the most thrombogenic (Fig. 10). This technique provides greater insight into the mechanisms of surface-induced thrombosis, but is qualitative in nature, as opposed to the more quantitative radiotracer methods. The results for $PDMS^{ox}$–$O_3Si(CH_2)_3(OCH_2CH_2)_3OCOCH_3$ were comparable to $PDMS^{ox}$–$O_3Si(CH_2)_{11}CO_2CH_3$. The alkyl-ester terminated surface $PDMS^{ox}$–$O_3Si(CH_2)_{11}CO_2CH_3$ showed a base layer of pseudopodial platelets, along with regions of extensive complex mural thrombi formation, after only 5 min of blood exposure (Fig. 10a). At 15 min, this material again showed regions of spreading platelets, and mural thrombi, with visible platelets, fibrin, leukocytes, and entrapped erythrocytes (Fig. 10b). At 30 min of blood exposure, a base layer of fully spread platelets was observed, along with some small (20 μm) white thrombi (Fig. 10c), and more large clots, again with visible platelets, fibrin, leukocytes, and entrapped erythrocytes. At 60 min of blood contacting time, most of the thrombi had embolized, so only smaller (50 μm) white thrombi were observed on a monolayer of pseudopodial platelets (Fig. 10d).

$PDMS^{ox}$–$O_3Si(CH_2)_{11}S(CH_2)_3(OCH_2CH_2)_3OH$ appeared to be somewhat less thrombogenic than the ester-terminated materials. Again, this result is more qualitative than that shown in Figures 8 and 9, and is

TABE III
Platelet and Fibrinogen Deposition Statistics Relative Rank

Material	Platelet Rank	Fibrinogen Rank
$PDMS^{ox}$–$O_3Si(CH_2)_2(CF_2)_7CF_3$	2.9 ± 1.1	2.8 ± 1.5
$PDMS^{ox}$–$O_3Si(CH_2)_{11}CO_2CH_3$	6.2 ± 0.9	5.6 ± 1.9
$PDMS^{ox}$–$O_3Si(CH_2)_9CH_3$	2.3 ± 1.1	2.3 ± 1.3
$PDMS^{ox}$–$O_3Si(CH_2)_3(OCH_2CH_2)_3OCOCH_3$	6.2 ± 0.8	5.7 ± 1.8
$PDMS^{ox}$–$O_3Si(CH_2)_{11}S(CH_2)_3(OCH_2CH_2)_3OH$	5.6 ± 0.7	4.8 ± 1.7
PE	2.1 ± 1.1	4.0 ± 1.6
Silastic pump grade tubing	2.7 ± 1.3	2.8 ± 1.3

dependent on the time points and surface regions analyzed. At 5 min of blood exposure, the platelet lawn varied from a submonolayer of pseudopodial platelets to a monolayer of more activated, fully spread platelets, with a second layer of pseudopodial platelets on top (Fig. 11a). After 15 min, a monolayer of pseudopodial platelets with small (20 μm) white thrombi and numerous adherent leukocytes (Fig. 11b) was observed. At 30 min, the thrombi had embolized, leaving behind a lawn of pseudopodial platelets (Fig. 11c). After an hour, the platelet lawn was still present, with monolayer regions of spread and unspread leukocytes. Further, macroscopic mural thrombi were also present at this time (Fig. 11d).

$PDMS^{ox}$–$O_3Si(CH_2)_9CH_3$ and $PDMS^{ox}$–$O_3Si(CH_2)_2(CF_2)_7CF_3$ had low levels of platelet activation and thrombus formation, and were largely equivalent. For $PDMS^{ox}$–$O_3Si(CH_2)_9CH_3$, a lawn of pseudopodial platelets was all that was observed after 5 and 15 min of blood exposure (Fig. 12a and b). Small (20 μm) white thrombi were seen at 30 min of blood-contacting time (Fig. 12c). At 60 min, a monolayer of

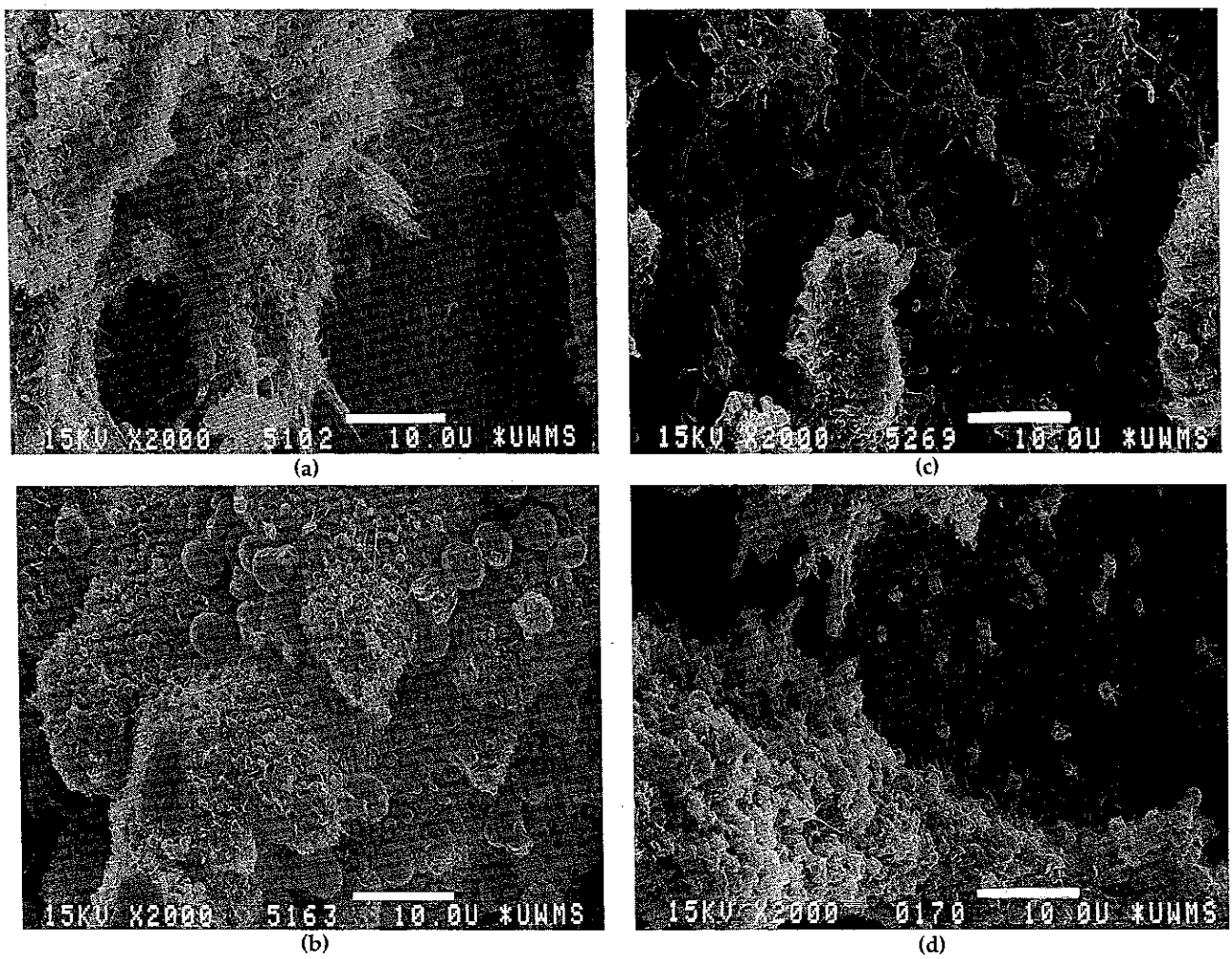

Figure 10. Scanning electron micrographs of $PDMS^{ox}$–$O_3Si(CH_2)_{11}CO_2CH_3$ after (a) 5 min; (b) 15 min; (c) 30 min; and (d) 60 min of blood exposure. (Scale bar = 10 μm).

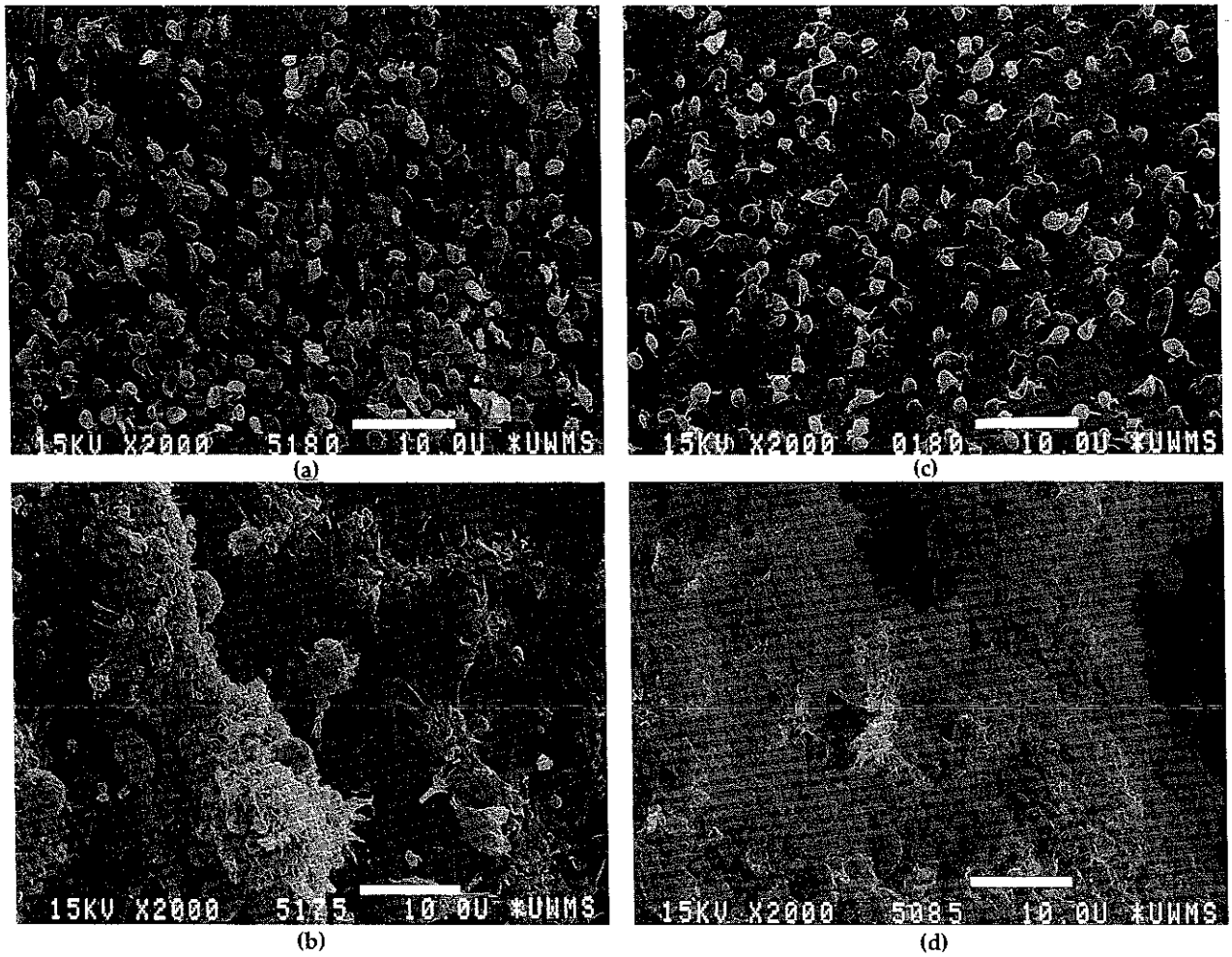

Figure 11. Scanning electron micrographs of PDMS^{ox}–$O_3Si(CH_2)_{11}S(CH_2)_3(OCH_2CH_2)_3OH$ after (a) 5 min; (b) 15 min; (c) 30 min; and (d) 60 min of blood exposure. (Scale bar = 10 μm.)

pseudopodial platelets was seen, along with monolayer regions of spread and unspread leukocytes (Fig. 12d).

CONCLUSIONS

Evaluation of the hemocompatibility of the surface-modified silastic tubing using a canine *ex vivo* series shunt experiment showed that PDMS^{ox}–$O_3Si(CH_2)_{11}CO_2CH_3$ and PDMS^{ox}–$O_3Si(CH_2)_{11}S(CH_2)_3(OCH_2CH_2)_3OH$ are the most thrombogenic. Since these groups were chosen in part to probe the role of surface hydrophilicity, it does not appear that the hydrophilicity of the chains plays a significant role in artificial-surface-induced thrombosis in this case. However, the ethylene oxide chain lengths used in the current study were much shorter than those used by other investigators, and may also be too densely packed to have the high mobility which is hypothesized to reduce protein adsorption and cellular adhesion.[26,43,44] It is possible that such short chain ethylene oxide groups may lack the high mobility seen by other investigators. Since large differences in thrombogenicity are seen when comparing PDMS^{ox}–$O_3Si(CH_2)_{11}CO_2CH_3$ with PDMS^{ox}–$O_3Si(CH_2)_3(OCH_2CH_2)_3OCOCH_3$, this suggests that the terminal esters are not the sole determinant of biocompatibility, but that subsurface groups also play a role in this case. The hypothesis that PDMS^{ox}–$O_3Si(CH_2)_3(OCH_2CH_2)_3OCOCH_3$ and PDMS^{ox}–$O_3Si(CH_2)_{11}S(CH_2)_3(OCH_2CH_2)_3OH$ might reduce platelet and protein adhesion was not supported. The best materials studied were surfaces grafted with methyl and perfluoromethyl functional groups. This result suggests that the most hydrophobic surfaces are the most hemocompatible. These materials were comparable to silicone rubber and polyethylene controls, both of which show low levels of platelet and fibrinogen deposition in the canine *ex vivo* model.

To further improve the blood compatibility of these SAMs, many ideas suggest themselves. First, if the surface density of ethylene oxide groups is decreased, their mobility may be increased. This could be done by forming mixed monolayers of methyl and

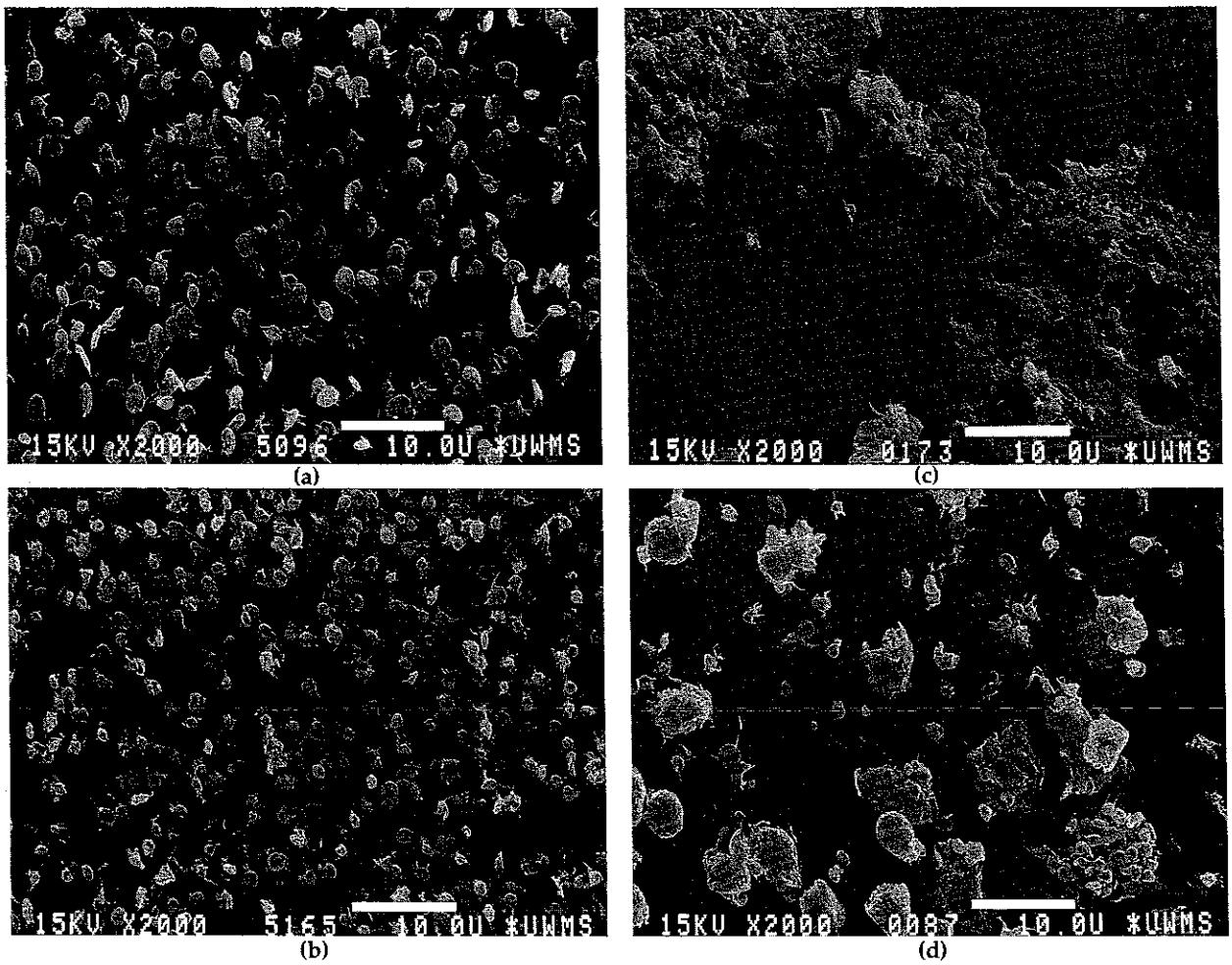

Figure 12. Scanning electron micrographs of PDMS^{ox}–$O_3Si(CH_2)_9CH_3$ after (a) 5 min; (b) 15 min; (c) 30 min; and (d) 60 min of blood exposure. (Scale bar = 10 μm.)

ethylene oxide groups. It may also be possible to alter the length of ethylene oxide groups in the self-assembled monolayer. Further, variation of the chemical composition of the head group may prove valuable. Self-assembled monolayers of sulfonate groups may have antithrombotic behavior similar to that seen for sulfonated polyurethanes.[2,32] SAMs of phosphonate groups may mimic cell membranes and therefore be thromboresistant.[45,46] Using this approach, it is possible carefully, and in a controlled way, to alter the surface chemistry of a material, thus influencing its blood-contacting properties.

Technical assistance was provided by Steve Smith (animal surgery and scanning electron spectroscopy), Arlene P. Hart (hematology). This work was supported in part by the National Institutes of Health, through Grants HL-24046 and HL-47179, and the Dow Corning Corp., Midland, Michigan.

References

1. B. J. Tyler, B. D. Ratner, D. G. Castner, and D. Briggs. "Variations between Biomer lots. I. Significant differences in the surface chemistry of two lots of a commercial poly(etherurethane)," *J. Biomed. Mater. Res.*, **26**, 273–289 (1992).
2. J. H. Silver, K. B. Lewis, B. D. Ratner, and S. L. Cooper, "The effect of polyol type on the surface structure of sulfonate-containing polyurethanes," *J. Biomed. Mater. Res.*, **27**, 735–745 (1993).
3. Y. S. Yeh, Y. Iriyama, Y. Matsuzawa, S. R. Hanson, and H. Yasuda, "Blood compatibility of surfaces modified by plasma polymerization," *J. Biomed. Mater. Res.*, **22**, 795–818 (1988).
4. G. Clarotti, A. A. B. Aoumar, F. Schue, J. Sledz, K. E. Geckeler, D. Flosch, and A. Orsetti, "Modification of membrane surfaces by plasma deposition of thin fluorocarbon films without affecting bulk properties," *Makromol. Chem.*, **192**, 2581–2590 (1991).
5. B. D. Ratner, "Plasma deposition for biomedical applications: A brief review," *J. Biomat. Sci. Polym. Edn.*, **4**, 3–11 (1992).
6. C. S. Dulcey, J. H. Georger, Jr., V. Krauthamer, D. A. Stenger, T. L. Fare, and J. M. Calvert, "Deep UV photochemistry of chemisorbed monolayers: Patterned coplanar molecular assemblies," *Science*, **252**, 551–554 (1991).
7. E. B. Troughton, C. D. Bain, G. M. Whitesides, R. G. Nuzzo, D. L. Allara, M. D. Porter, "Monolayer films prepared by the spontaneous self-assembly of sym-

metrical and unsymmetrical dialkyl sulfides from solution onto gold substrates: Structure, properties and reactivity of constituent functional groups," *Langmuir*, **4**, 365–385 (1988).
8. C. D. Bain and G. M. Whitesides, "Molecular-level control over surface order in self-assembled monolayer films of thiols on gold," *Science*, **240**, 62–63 (1988).
9. C. D. Bain, Ph.D. thesis, Harvard University, 1988.
10. R. G. Nuzzo, and D. L. Allara, "Adsorption of bifunctional organic disulfides on gold surfaces," *J. Am. Chem. Soc.*, **105**, 4481–4483 (1983).
11. M. Collinson, E. Bowden, and M. J. Tarlov, "Voltammetry of covalently immobilized cytochrome c on self-assembled monolayer electrodes," *Langmuir*, **8**, 1247–1250 (1992).
12. J. Sagiv, "Organized monolayer by adsorption. I. Formation and structure of oleophobic mixed monolayer on solid surfaces," *J. Am. Chem. Soc.*, **102**, 92 (1980).
13. R. Maoz and J. Sagiv, "The formation and structure of self-assembling monolayers. I. A comparison ATR-wettability study of Langmuir-Blodgett and adsorbed films on flat substrates and glass microbeads," *J. Colloid Interface Sci.*, **100**, 465 (1984).
14. S. R. Wasserman, Y.-T. Tao, and G. M. Whitesides, "Structure and reactivity of alkylsiloxane monolayer formed by reaction of alkyl trichlorosilane on silicon substrate," *Langmuir*, **5**, 1074 (1989).
15. N. Tillman, A. Ulman, J. S. Schildkraut, and T. C. Penner, "Incorporation of phenoxy groups in self-assembled monolayers of trichlorosilane derivatives: Effects on film thickness, wettability, and molecular orientation," *J. Am. Chem. Soc.*, **110**, 6136–6144 (1988).
16. S. K. Bhatia, J. L. Teixeira, M. Anderson, L. C. Shriver-Lake, J. M. Calvert, J. M. Georger, J. J. Hickman, C. S. Dulcey, P. E. Schoen, and F. S. Ligler, "Fabrication of surfaces resistant to protein adsorption and application to two-dimensional protein patterning," *Anal. Biochem.*, **208**, 197–205 (1993).
17. K. Lewandowska, E. Pergament, C. N. Sukenik, and L. A. Culp, "Cell-type-specific adhesion mechanisms mediated by fibronectin adsorbed to chemically derivatized substrata," *J. Biomed. Mater. Res.*, **26**, 1343–1363 (1992).
18. M. K. Chaudhury and G. M. Whitesides, "Direct measurement of interfacial interactions between semispherical lenses and flat sheets of poly(dimethylsiloxane) and their chemical derivatives," *Langmuir*, **7**, 1013–1025 (1991).
19. M. K. Chaudhury and M. J. Owen, "Correlation between adhesion hysteresis and phase state of monolayer films," *J. Phys. Chem.*, **97**, 5722–5726 (1993).
20. G. S. Ferguson, M. K. Chaudhury, H. A. Biebuyck, and G. M. Whitesides, "Monolayers on disordered substrates: Self-assembly of alkyltrichlorosilanes on surface-modified polyethylene and poly(dimethylsiloxane)," *Macromolecules*, **26**, 5870–5875 (1993).
21. D. A. Stenger, J. H. Georger, C. S. Dulcey, J. J. Hickman, A. S. Rudolph, T. B. Nielsen, S. M. McCort, and J. M. Calvert, "Coplanar molecular assemblies of amino- and perfluorinated alkylsilanes: Characterization and geometric definition of mammalian cell adhesion and growth." *J. Am. Chem. Soc.*, **114**, 8435–8442 (1992).
22. K. L. Prime and G. M. Whitesides, "Self-assembled organic monolayers: Model systems for studying adsorption of proteins at surfaces," *Science*, **252**, 1164–1167 (1991).
23. J. Frommer, R. Luthl, E. Meyer, D. Anselmetti, M. Dreler, R. Overney, H.-J. Guntherodt, and M. Fujihira, "Adsorption at domain edges," *Nature*, **364**, 198 (1993).
24. X.-H. Yu, A. Z. Okkema, and S. L. Cooper, "Synthesis and physical properties of poly(fluoroalkylether)-urethanes," *J. Appl. Polym. Sci.*, **41**, 1777–1795 (1990).
25. D. K. Han, S. Y. Jeong, Y. H. Kim, and B. G. Min, "Surface characteristics and blood compatibility of polyurethanes grafted by perfluoroalkyl chains," *J. Biomater. Sci. Polym. Edn.*, **3**, 229–241 (1992).
26. D. Kiaei, A. S. Hoffman, B. D. Ratner, and T. A. Horbett, "Interaction of blood with gas discharge treated vascular grafts," *J. Appl. Poly. Sci.: Appl. Polym. Symp.*, **42**, 269–283 (1988).
27. J. L. Bohnert, B. C. Fowler, T. A. Horbett, and A. S. Hoffman, "Plasma gas discharge deposited fluorocarbon polymers exhibited reduced elutability of adsorbed albumin and fibrinogen," *J. Biomat. Sci. Polym. Ed.*, **1**, 279 (1990).
28. A. M. Garfinkle, A. S. Hoffman, B. D. Ratner, L. O. Reynolds, and S. R. Hanson, "Effects of a tetrafluoroethylene glow discharge on patency of small diameter dacron vascular grafts," *Trans. ASAIO*, **30**, 432–439 (1984).
29. K. D. Park, T. Okano, C. Nojiri, and S. W. Kim, "Heparin immobilization on segmented polyurethaneurea surfaces—effect of hydrophilic spacers," *J. Biomed. Mater. Sci.*, **22**, 977–992 (1988).
30. E. Brinkman, A. Poot, L. van der Does, and A. Bantjes, "Platelet deposition studies on copolyetherurethanes modified with poly(ethylene oxide)," *Biomaterials*, **11**, 200–205 (1990).
31. E. W. Merrill and E. W. Salzman, "Polyethylene oxide as a biomaterial," *ASAIO J.*, **6**, 60–64 (1983).
32. D. K. Han, S. Y. Jeong, Y. H. Kim, B. G. Min, and H. I. Cho, "Negative cilia concept for thromboresistance: Synergistic effect of PEO and sulfonate groups grafted onto polyurethanes," *J. Biomed. Mater. Res.*, **25**, 561–575 (1991).
33. B. J. Tyler, D. G. Castner, and B. D. Ratner, "Regularization: A stable and accurate method for generating depth profiles from angle-dependent XPS data," *Surf. Interface Anal.* **14**, 443–450 (1989).
34. M. P. Seah and W. A. Dench, "Quantitative electron spectroscopy of surfaces: A standard data base for electron inelastic mean free path in solids," *Surf. Interface Anal.* **1**, 2–11 (1979).
35. M. D. Lelah, T. G. Grasel, J. A. Pierce, and S. L. Cooper, "The measurement of contact angles on circular tubing surfaces using the captive bubble technique," *J. Biomed. Mater. Res.*, **19**, 1011–1015 (1985).
36. M. D. Lelah, L. K. Lambrecht, and S. L. Cooper, "A canine *ex vivo* series shunt for evaluating thrombus deposition on polymer surfaces," *J. Biomed. Mater. Res.*, **18**, 475–496 (1984).
37. T. G. Grasel and S. L. Cooper, "Properties and biological interactions of polyurethane anionomers: Effect of sulfonate incorporation," *J. Biomed. Mater. Res.*, **23**, 311–338 (1989).
38. K. Park, D. F. Mosher, and S. L. Cooper, "Acute surface-induced thrombosis in the canine *ex vivo* model: Importance of protein composition of the initial monolayer and platelet activation," *J. Biomed. Mater. Res.* **20**, 589–612 (1986).
39. A. Zanker, "Detection of outliers by means of Nalimov's test," *Chem. Eng.*, **91**(16), 74 (1984).
40. S. R. Wasserman, Ph.D. thesis, Harvard University, 1989.

41. A. Takahara, A. Z. Okkema, S. L. Cooper, and A. J. Coury, "Effect of surface hydrophilicity on ex vivo blood compatibility of segmented polyurethanes," *Biomaterials*, **12**, 324–334 (1991).
42. T. G. Grasel and S. L. Cooper, "Surface properties and blood compatibility of polyurethaneureas," *Biomaterials*, **7**, 315–328 (1986).
43. N. P. Desai and J. A. Hubbell, "Solution technique to incorporate polyethylene oxide and other water-soluble polymers into surfaces of polymeric biomaterials," *Biomaterials*, **12**, 144–153 (1991).
44. N. P. Desai and J. A. Hubbell, "Biological responses to polyethylene oxide modified polyethylene terephthalate surfaces," *J. Biomed. Mater. Res.*, **25**, 829–843 (1991).
45. J. A. Hayward and D. Chapman, "Biomembrane surfaces as models for polymer design: The potential for hemocompatibility," *Biomaterials*, **5**, 135–142 (1984).
46. R. F. A. Zwaal and E. M. Bevers, "Platelet phospholipid asymmetry and its significance in hemostasis," in *Subcellular Biochemistry*, (D. B. Roodyn, ed.), Plenum Press, New York, (1983), pp. 299–334.

Received January 7, 1994
Accepted November 10, 1994